

Polarization and Resonance Properties of Magnetic X-Ray Scattering in Holmium

Doon Gibbs

Brookhaven National Laboratory, Upton, New York 11973

D. R. Harshman, E. D. Isaacs, and D. B. McWhan

AT&T Bell Laboratories, 600 Mountain Avenue, Murray Hill, New Jersey 07974

D. Mills

Cornell High Energy Synchrotron Source, Cornell University, Ithaca, New York 14853

and

C. Vettier

Institut Laue-Langevin, 38042 Grenoble, Cedex, France

(Received 15 June 1988)

By measuring the degree of linear polarization we identify the orbital and spin contributions to the x-ray magnetic scattering in holmium. When the incident x-ray energy is tuned through the L_{III} absorption edge, we observe a fiftyfold resonant enhancement of the magnetic signal, and resonant integer harmonics. The line shapes of the two linear components scattered parallel and perpendicular to the diffraction plane are distinct in energy with a 6-eV splitting.

PACS numbers: 75.25.+z, 75.50.Ee, 78.70.Ck

The cross section for the scattering of x rays from condensed matter contains terms which depend on the electronic spin and orbital angular momentum densities.¹⁻⁴ For typical x-ray energies, the amplitudes for these terms are smaller than those for the usual charge (or Thomson) scattering by a factor $(\hbar\omega/mc^2) \sim 0.02$. As a result of the coupling of the incident x ray to both the electronic charge and its magnetic moment, the polarization dependence of the orbital magnetization density differs from that of the spin density (in contrast to neutron diffraction, where they are identical).^{3,5} In this paper we explore the polarization and energy dependence of the x-ray-scattering cross section of the spiral antiferromagnet holmium, as the incident x-ray energy is tuned near to and far from the L_{III} absorption edge.

In the limit of high energies, the x-ray magnetic scattering has the form $[\mathbf{L}(K) \cdot \mathbf{A} + \mathbf{S}(K) \cdot \mathbf{B}]$, where $\mathbf{L}(k)$ and $\mathbf{S}(K)$ are the atomic orbital and spin magnetization densities, and \mathbf{A} and \mathbf{B} are polarization vectors determined by the geometry.⁵ Off resonance (i.e., 200 eV below the edge), we measure the degree of linear polarization of the x-ray magnetic scattering and use this formula to identify the orbital and spin contributions to the cross section. These techniques should be of interest in quantitative studies of mixed-valence and heavy-fermion material, where the $4f$ and $5f$ spin and orbital distributions are presently uncertain.

Near an absorption edge there are additional resonant contributions which dominate the magnetic scattering.⁶ For incident energies near the L_{III} edge, we observe a fiftyfold resonant enhancement of the cross section at $(0,0,2+\tau)$, where τ is the wave vector for the magnetic

spiral. In addition, we observe resonant second, third, and fourth harmonics, located at $2+2\tau$, $2+3\tau$, and $2+4\tau$. For the first two harmonics, the line shapes of the linearly polarized components scattered parallel and perpendicular to the diffraction plane are distinct in energy, with a 6-eV splitting, which leads to substantial changes in the degree of linear polarization at resonance. For the third and fourth harmonics no splitting is observed. In the following Letter⁶ a theory is developed which explains this remarkable behavior on the basis of electric multiple transitions to $4f$ and $5d$ levels with sensitivity to the magnetization arising from exchange effects. Similar enhancements should occur in transition elements and in the actinide series. In addition, resonance techniques may permit studies of two-dimensional magnetic ordering with existing synchrotron sources, with possible applications to high- T_c superconductors. Finally, we note that the first suggestion that interesting magnetic effects might occur near an absorption edge was made by Blume.³ Namikawa *et al.*⁷ performed early measurements of resonant magnetic effects in ferromagnetic Ni.

Metallic holmium has ten $4f$ electrons in a 5I_8 ground state. The L_{III} absorption edge occurs at 8.067 keV, and is well separated from its L_{II} and L_I partners at 8.916 and 9.395 keV, respectively. Below the magnetic ordering temperature $T_N = 133$ K, the diffraction pattern consists of single pairs of magnetic satellites split symmetrically around each main Bragg reflection (parallel to the c axis), consistent with a simple spiral modulation. The magnetic wave vector τ decreases with decreasing temperature, from $\tau \sim 0.30c^*$ at 130 K to $\tau = \frac{1}{6}c^*$ at 10 K,

and may lock to rational values. Besides the principal magnetic scattering observed at τ , weak fifth and seventh magnetic harmonics, arising from distortions of the spiral by the crystal field, also occur.^{8,9}

Synchrotron radiation is predominantly linearly polarized within the plane of the electron orbit and elliptically polarized above and below the plane. The degree of linear polarization is defined as $P = (I_{\perp} - I_{\parallel}) / (I_{\perp} + I_{\parallel})$, where I_{\perp} and I_{\parallel} are the intensities of the linear components polarized perpendicular and parallel to the diffraction plane (see inset, Fig. 1). With the sample centered on the orbit plane, the right- and left-circular components cancel in the scattered beam, and P is determined by the angular acceptance of the defining slits and the size and fluctuations of the source. The degree of linear polarization P' for the magnetic scattering at τ from a spiral⁵ is

$$\begin{aligned}
 P' &= (I'_{\perp} - I'_{\parallel}) / (I'_{\perp} + I'_{\parallel}); \\
 I'_{\perp} &= (1 + P) + (1 - P)(1 + g)^2 \sin^2 \theta, \\
 I'_{\parallel} &= (1 + P)(1 + g)^2 \sin^2 \theta + (1 - P)(1 + 2g \sin^2 \theta)^2, \\
 g(K) &= \frac{\mathbf{L}(K) \cdot \mathbf{J}(K)}{\mathbf{S}(K) \cdot \mathbf{J}(K)} = \frac{(\mathbf{L} \cdot \mathbf{J})f_L(K)}{(\mathbf{S} \cdot \mathbf{J})f_S(K)}.
 \end{aligned}
 \tag{1}$$

Here, θ is half the scattering angle and $g(K)$ is the ratio of the atomic orbital and spin magnetization densities, each projected along the total angular momentum \mathbf{J} . For holmium $g(K)$ may be rewritten in terms of the normalized orbital and spin form factors: $g(K) = 3[f_L(K)/f_S(K)]$.¹⁰ Equation (1) is derived for incident x-ray energies much greater than any excitation energy of the solid. Dispersive corrections to the magnetic scattering 200 eV below the edge are assumed to be small.

The experiments were begun on beam line X16B at the National Synchrotron Light Source (NSLS); the data reported here were obtained on the wiggler station A-2 at the Cornell High Energy Synchrotron Source (CHESS). The Ho sample, grown at Ames Laboratory by B. Beaudry, was supported inside a closed-cycle helium refrigerator which was mounted on a standard four-circle diffractometer. Its $9 \times 4\text{-mm}^2$ (001) face (mosaic width 0.03°) was studied in vertical reflection geometry with a sagittally focused two-crystal Si(111) monochromator. The incident degree of linear polarization P was monitored continuously by means of a Be-foil Compton polarimeter¹¹ designed by W. Schildekamp at CHESS. To measure the linear components of the scattered beam, a pyrolytic-graphite crystal (mosaic width 0.3°) was placed after the sample (see inset, Fig. 1). When the incident x-ray energy is tuned to $E = 7.847$ keV, the scattering angle for the pyrolytic-graphite (006) reflection is 90° , and one linear component is reflected, while the other is suppressed. By our rotating the graphite 90° about the axis of the scattered beam, the former is suppressed and the latter is reflected (see inset, Fig. 1).^{8,12} Because

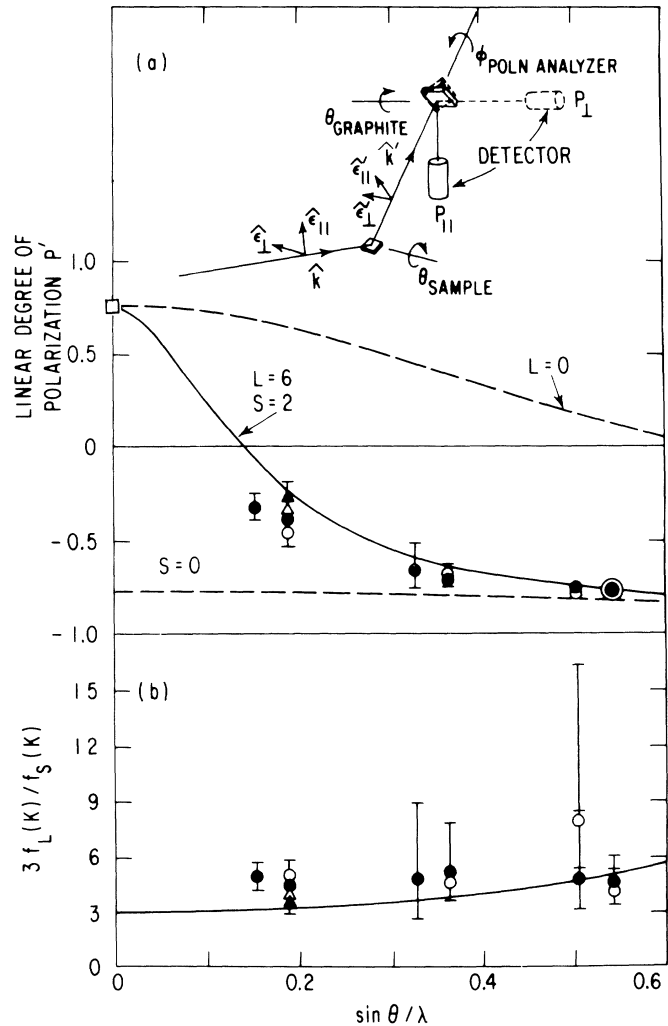


FIG. 1. Inset: Scattering geometry, including polarization analysis. The vertical diffraction plane is spanned by \mathbf{k} and \mathbf{k}' . (a) Off-resonant linear degree of polarization P' for the magnetic scattering at $(l + \tau)$ plotted vs momentum transfer. Open circles indicate the results obtained by rocking of the graphite analyzer at the magnetic peak and in the background. Filled circles were obtained by rocking of the sample for fixed analyzer angle (and correcting for the small differences in horizontal and vertical divergence at each reflection). Open and filled triangles refer to the results obtained from a Ge(111) analyzer in place of the graphite. The solid line shows P' calculated from Eq. (1) with form factors calculated in Ref. 10. At $\theta=0$ (open square) the value of P' corresponds to the average incident degree of linear polarization, $P=0.77$. The dashed lines show P' calculated first assuming $L=0$ (upper), and then assuming $S=0$ (lower). (b) The measured ratio $g(K)$ of orbital and spin form factors obtained by inversion of Eq. (1). The solid line gives $g(K)$ calculated from Ref. 10.

of the differing horizontal and vertical angular divergences of the scattered beam, integrated intensity measurements may require the rocking of both the sample and the analyzer crystal (see caption, Fig. 1).

Figure 1(a) shows the off-resonance ($E = 7.847$ keV) measurements of P' at the positive and negative magnetic satellites, $\tau = \pm \frac{1}{6}$, of the (002), (004), and (006) Bragg reflections. The error bars reflect the uncertainty arising from the large background (due to charge scattering) in the weaker, perpendicular component. The solid line shows P' calculated from Eq. (1) with calculated form factors for $g(K)$ (Ref. 10) and the assumption of $P = 0.77$. This value of P , reliable to within 15%, is the average obtained from measurements of the direct beam with the Compton polarimeter and from measurements of the charge scattering at the (002), (004), and (006) reflections with the graphite analyzer.

It is clear from the figure that the incident polarization is rotated upon magnetic scattering, from mainly perpendicular to the diffraction plane at $\theta = 0$ ($P' = P = 0.77$) to mainly parallel at the $(0,0,6+\tau)$ reflection ($P' \approx -0.8$). To within the experimental error, this behavior is consistent with Eq. (1) and reflects the dependence of the orbital magnetization density on $\sin^2\theta$. This is illustrated in Fig. 1(a) by the plots of P' with $L = 0$ and $S = 0$. In Fig. 1(b) we compare the measured ratio $g(K)$ of orbital and spin form factors to the ratio calculated with use of nonrelativistic Hartree-Fock wave functions. At $K = 0$ the calculated ratio (solid line) equals 3.0, and increases with increasing K , reflecting the more rapid falloff of the spin form factor in holmium. As may be seen, however, the experimental error approximately spans this variation in Q . Significant improvements are possible by the increase of the signal-to-noise ratio in the perpendicular component and by the increase of the degree of linear polarization of the incident beam [see Eq. (1)].

An important result of the present study is the discovery of a fiftyfold resonant enhancement of the magnetic scattering as the incident x-ray energy is tuned through the L_{III} absorption edge. For an incident flux of $\sim 10^{11}$ photons/s we observe a scattered signal of ~ 70000 counts/s at the $(0,0,2+\tau)$ reflection. In addition, we observe resonant second-, third-, and fourth-order harmonics, reduced in intensity from the first at 8.065 keV in the ratios

$$I(2+2\tau):20I(2+2\tau):150I(2+3\tau):300I(2+4\tau).$$

The energy dependence of the intensities scattered parallel and perpendicular to the diffraction plane at τ , 2τ , and 3τ is shown in Fig. 2. The data have been normalized by μ to correct for the absorption. The solid vertical line indicates the energy of the edge, which we have taken as the inflection point of the abrupt change in absorption at 8.067 keV. In each case the line shapes of the two components are distinct, peaking ≈ 3 eV above or below the edge. The fine structure, however, depends on harmonic order. For the scattering at τ , the parallel component is always stronger and peaks above the edge, while the perpendicular component peaks below. Both

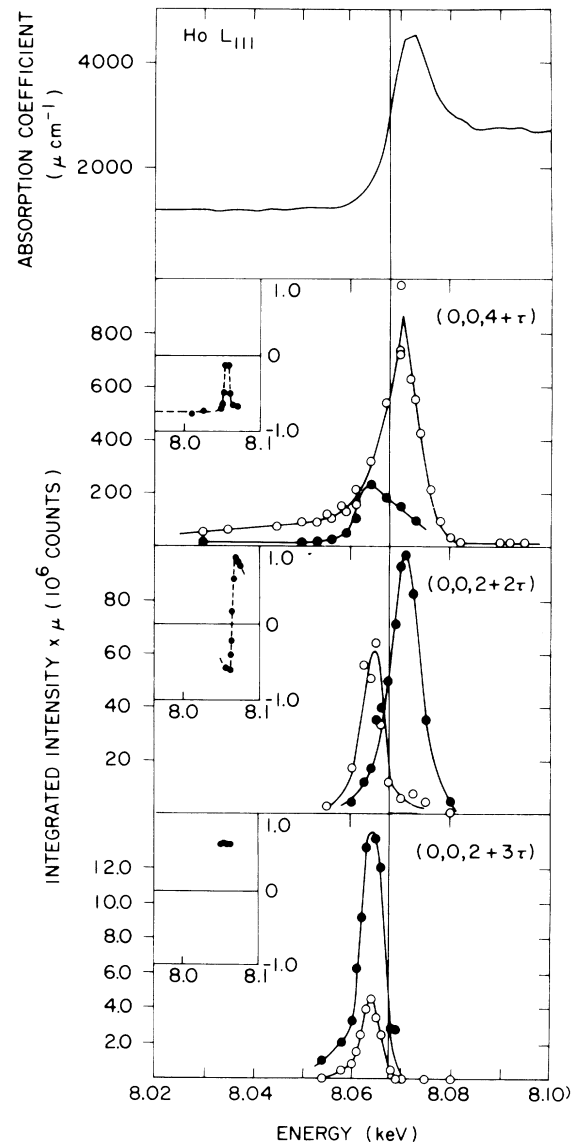


FIG. 2. Top: Measured absorption coefficient plotted vs incident x-ray energy for the L_{III} edge of holmium. Lower: Integrated intensities plotted vs energy for the linear components scattered parallel (open circles) and perpendicular (filled circles) to the diffraction plane at τ , 2τ , and 3τ . Lines are drawn only to guide the eye. Polarization analysis was performed at the $(0,0,4+\tau)$ below 20 K, where $\tau = (1/6)c^*$, and at the $(0,0,2+2\tau)$ and $(0,0,2+3\tau)$ at 25 K, where $\tau = (0.186)c^*$. At the $(0,0,2+4\tau)$ resonant scattering was observed only below the edge. Insets, lower: Corresponding degree of linear polarization plotted vs energy. Solid vertical line indicates energy of L_{III} edge.

components appear asymmetric. At 2τ , the parallel component peaks below the edge, while the perpendicular peaks above. At 3τ , both components peak below the edge and no scattering is observed above. This structure is succinctly displayed in a plot of the energy dependence of the degree of linear polarization P' , which is shown in-

set in each panel of the figure. For the magnetic scattering at τ , P' undergoes a resonance ≈ 3 eV below the edge, suggesting that at this energy the scattering is either circularly polarized or unpolarized. In contrast, for the scattering at 2τ , the polarization is parallel to the diffraction plane below the edge ($P' \approx -0.7$) and perpendicular above ($P' \approx 0.7$). For 3τ , $P' \approx 0.6$ is independent of energy below the edge.

According to the theory developed in the following Letter,⁶ the parallel and perpendicular components of the harmonics observed below the edge in Fig. 2 correspond to electric quadrupole transitions from $2p$ core states to $4f$ band states near E_F . Similarly, above the edge, the observation of parallel and perpendicular components at τ and 2τ (and no higher harmonics) corresponds to electric dipole transitions from $2p$ and $5d$ levels. The observed asymmetry in the magnetic scattering at τ follows from interference of the resonant and non-resonant contributions near the edge. The possibility that electric multipole transitions may give rise to magnetic scattering is a consequence of the exclusion principle. In this way the resonant scattering is sensitive to magnetization in the f and d bands, and should lead to a new spectroscopy of magnetic states in rare-earth, actinide, and transition elements. We conclude by noting that we have also observed weaker resonances in the magnetic scattering at the L_I and L_{II} absorption edges and an apparent increase in linewidth at the L_{III} edge. These results will be given in a full paper.

We have benefitted from discussions with J. D. Axe, B. W. Batterman, M. Blume, J. W. Davenport, J. P. Hannon, P. M. Platzman, G. T. Trammell, and G. K.

Wertheim. The work at Brookhaven National Laboratory is supported by the U.S. Department of Energy under Contract No. DE-AC02-76CH00016. CHESS is supported by the National Science Foundation under Grant No. DMR-84112465.

¹P. M. Platzman and N. Tzoar, Phys. Rev. B **2**, 3556 (1970).

²F. deBergevin and M. Brunel, Acta Crystallogr. A **37**, 314-324 (1981).

³M. Blume, J. Appl. Phys. **57**, 3615 (1985).

⁴O. L. Zhizhimov and I. B. Khriplovich, Zh. Eksp. Teor. Fiz. **87**, 547 (1984) [Sov. Phys. JETP **60**, 313 (1984)].

⁵M. Blume and D. Gibbs, Phys. Rev. B **37**, 1779 (1988).

⁶J. P. Hannon, G. T. Trammell, M. Blume, and D. Gibbs, following Letter [Phys. Rev. Lett. **61**, 1245 (1988)].

⁷K. Namikawa, M. Ando, T. Nakajima, and H. Kawata, J. Phys. Soc. Jpn. **54**, 4099 (1985).

⁸D. Gibbs, D. E. Moncton, K. L. D'Amico, J. Bohr, and B. Grier, Phys. Rev. Lett. **55**, 234 (1985); J. Bohr, D. Gibbs, D. E. Moncton, and K. L. D'Amico, Physica (Amsterdam) **140A**, 349 (1986).

⁹*Handbook on the Physics and Chemistry of Rare Earth Metals*, edited by K. A. Gschneider and L. Eyring (North-Holland, Amsterdam, 1978), Vol. 1.

¹⁰M. Blume, A. J. Freeman, and R. E. Watson, J. Chem. Phys. **37**, 1242 (1962), and **41**, 1878 (1964).

¹¹G. Materlick and P. Suortti, J. Appl. Crystallogr. **17**, 7 (1984); F. Smend, D. Schaupp, H. Czerwinski, A. H. Millhouse, and H. Schenk-Strauss, Nucl. Instrum. Methods Phys. Res., Sec. A **242i**, 290 (1985).

¹²S. Chandrasekar, S. Ramasehan, and A. K. Singh, Acta Crystallogr. A **25**, 140 (1969).